Phys. Met. Metall. Vol. 68 No. 5, pp. 127–132, 1989
Printed in Great Britain

0031–918X/89 $10.00+.00

UDC 669.24'295'296 : 539.4.015

STRUCTURE, PROPERTIES AND GLASS-FORMING CAPACITY OF AMORPHOUS ALLOYS OF THE Ti_2Ni–Zr_2Ni SECTION OF THE Ti–Zr–Ni SYSTEM*

V. N. CHEBOTNIKOV, V. V. MOLOKANOV, Ye. B. RUBINA and Yu. K. KOVNERISTYY

Bykov Institute of Metallurgy, Academy of Sciences, U.S.S.R.

(*Received* 2 *June* 1988)

The structure and properties of amorphous and equilibrium crystalline alloys of the Ti_2Ni–Zr_2Ni section of the Ti–Zr–Ni system were investigated by the methods of X-ray diffraction analysis, differential thermal analysis (DTA), and resistance and microhardness measurements. The capacity of the alloys for glass formation was evaluated. The alloy in the eutectic range and formed by the interaction of intermetalloids ZrTiNi and Zr_2Ni was found to have the lowest critical cooling rate $R_c = 8.10^3$ K/sec. The influence of the ternary Laves phase in increasing the glass-forming capacity of alloys of that section is discussed.

The processes involved in the formation of amorphous alloys (AA) and the factors governing the capacity for glass formation can be ascertained from comparative physicochemical investigations of specimens in different structural states, ranging from completely disordered (amorphous state) to the equilibrium crystalline state [1]. Here the phase structure and properties of Ti–Zr–Ni alloys in the amorphous and crystalline states have been studied on the section between intermetalloids Ti_2Ni–Zr_2Ni.

The charge materials consisted of Ti VT1-00 in the form of 0·1 mm thick foil, iodide Zr and electrolytic Ni (99·90%). 20 g casts were melted in the LK-8 arc furnace with the non-consumable electrode and water-cooled copper base in purified helium atmosphere at 33 kPa. Each cast was remelted not less than five times. Weight, chemical analysis and density measurements were used to verify that the composition matched the theoretical formula (permissible deviation of not more than 0·2%). Some of the casts were used to produce rapidly quenched strip by spinning the melt in purified helium atmosphere. Others were used to study the microstructure, phase structure and microhardness. The cast alloys were annealed for 200 hr at 973 K in double-walled evacuated quartz ampoules with Zr getter, followed by cooling in water.

The amorphous and annealed crystalline alloys were analysed on the DRON-2 X-ray crystallographic apparatus using filtered FeK_α radiation and MoK_α radiation monochromatized with a graphite monochromater. The amorphous alloys (AA) were analysed in the vacuum high-temperature

* *Fiz. metal. metalloved.*, **68**, No. 5, 964–968, 1989.

attachment to the DRON-2 diffractometer using CuK_α radiation. Diffraction patterns were taken at 293, 623, 673, 733, 773, 823, 873, 973 K after continuous heating at 50 K/min. Photography was carried on for about 30 min at each temperature, at scanning rate 1°/min. Information regarding the short-range order structure was obtained from the diffraction data on the SM-4 computer using the method suggested in [2] for normalizing the intensity curves.

The thermal effects during melting of the crystalline alloys, together with the temperatures of the different stages of AA crystallization, were registered by means of differential thermal analysis (DTA) at a heating/cooling rate of 20 K/min in purified helium atmosphere on the DTA-5.

The specific electrical resistivity ρ was measured at room temperature with the standard four-probe method. For determination of the absolute values of ρ the accuracy of the measurements was improved by allowing for the geometrical factor [3] calculated from the mass, density and length of the specimens. The relative error of measurement was not more than 2%.

The microhardness of the annealed, cast and rapidly quenched alloys was measured on the PMT-3 under a load of 0·98 H. Each value was found as the arithmetical mean of not less than eight measurements. The relative error of microhardness measurement was 8%.

The method described in [4] was used to determine the dependence of embrittlement on the chemical composition of AA.

A method of braking the quenched disc similar to that described in [5], was used to determine the critical depth of the amorphous strip, i.e. the depth at which amorphization still occurs. The parameters of the process were varied for each specific composition by adjusting the thickness between 30 and 1200 μm. Following the recommendation of the authors of [5], the critical depth was taken as that at which the first precipitates of a crystalline phase on the free side of amorphous strip were observed in an optical microscope at a magnification of 100. The amorphous state was also verified by X-ray diffraction analysis.

The polythermal section Ti_2Ni–Zr_2Ni was constructed on the basis of the physicochemical analyses of cast and annealed Ti–Zr–Ni alloys (Fig. 1*a*). The structure features of that section are due to the interaction of the three intermetallic compounds:$Ti_2Ni(\delta)$, $Zr_2Ni(l)$, $ZrTiNi(\lambda_1)$. That eutectic section consists of two low-temperature eutectics crystallized in reactions $L \xrightarrow{1173K} \delta+\lambda_1$ and $L \xrightarrow{1123K} \lambda_1+l$. On the right and the left of the Laves phase in the central part there are two-phase regions. Although there is no Laves phase in binary systems Ti–Ni, Ti–Zr and Zr–Ni [6], a ternary Ti–Zr–Ni Laves phase of the $MgZn_2$ type is formed in the system TiZrNi with a wide range of homogeneity. The λ_1 phase in this section is formed coherently at 1193 K with a maximum at 30% Zr. The deviation of that maximum from stoichiometry seems to be due to imperfect size compatibility. The ZrTiNi Laves phase has a high level of hardness H_V = 7000–7300 MPa and is extremely brittle, which is due to the contribution of the covalence component to the energy of the chemical bond [7]. The homogeneity range of that phase contracts to somewhere between 21 and 30% Zr at 973 K.

The metastable diagram of the crystallization of AA of that section (Fig. 1*b*) was constructed on the basis of high-temperature X-ray diffraction analysis and DTA. It can be seen from that figure that the thermal stability of AA rises from 690 to 815 K when the Zr concentration is increased to 18%, and alloys of that concentration range crystallize in one stage with precipitation of the metastable compound $Ti_2Ni(\delta)$. AA in the range 18–47% Zr crystallized with precipitation of Laves phase $ZrTiNi(\lambda_1)$, with some loss of thermal stability. Where the Zr concentration is large, crystallization takes two

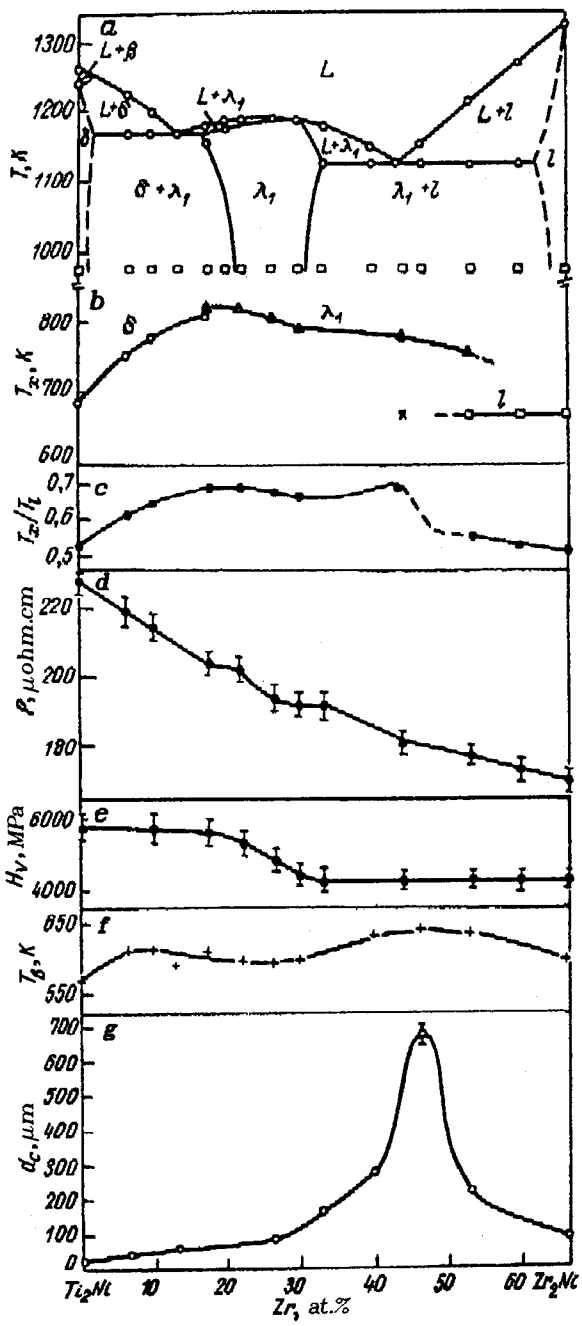

Fig. 1. Constitution diagram and composition vs properties curves of AA of the Ti_2Ni–Zr_2Ni section of system Ti—Zr—Ni: *a* —equilibrium diagram, *b* — curve of metastable crystallization of AA, *c* — T_x / T_l, *d* — specific resistivity of AA, *e* — microhardness of AA, *f* — brittle point of AA, *g* — critical depth of amorphous strip.

stages, starting with precipitation of a metastable phase based on compound $Zr_2Ni(l)$, followed by ZrTiNi. The AA corresponding to stoichiometric compounds Ti_2Ni, ZrTiNi and Zr_2Ni crystallize in one stage, with a pronounced and narrow exopeak on the DTA curve.

Figure 1*c* gives the results of our analysis of the glass-forming capacity of the alloys on the basis of the empirical criterion T_x / T_l (T_x – crystallization temperature, T_l – liquidus temperature). The T_x / T_l ratio for AA of that section has high values from 0·50 to 0·69 after which T_x / T_l = 0·45–0·66 [8] for most of the known AA. The lowest values, 0·53 and 0·50, were found for AA with Ti_2Ni and Zr_2Ni

stoichiometry, and the highest 0·64–0·69, for alloys corresponding to the range of primary crystallization of phase ZrTiNi.

When Zr substitutes Ti the resistivity (ρ) falls from 222 to 168 μOhm.cm (Fig. 1*d*). H_V the microhardness of Ti-based AA is 25% higher than for those based on Zr (Fig. 1*e*). On the concentration curves of the resistivity of microhardness of AA at 20–33% there is an inflection corresponding to the homogeneity range of Laves phase ZrTiNi on the equilibrium constitution diagram.

For AA in the intermetallic compound range the brittle point T_B (Fig. 1*f*) occurs at lower levels (575–600 K) than in the eutectic range (620–645 K). That appears to be due to changes in the chemical short-range order of AA in the process of annealing, which must be more marked on alloys corresponding to the stoichiometric composition.

The critical cooling rate R_c is known to be a quantitative parameter of the glass-forming capacity of AA (R_c is found from the critical depth of amorphous strips d_c [4]). According to Fig. 1*g* Laves phase ZrTiNi has the highest glass-forming capacity of intermetallic compounds of the section (Ti_2Ni, ZrTiNi, Zr_2Ni). The critical depth d_c increases when AA are further alloyed with intermetallic compounds. The biggest rise in d_c occurs when titanium are substituted by zirconium atoms in the ternary compound ZrTiNi. A sharp peak d_c=680 μm corresponding to the critical cooling rate $R_c = 8.10^3$ K/sec is observed in the range of the eutectic formed by compounds ZrTiNi and Zr_2Ni. A comparison of the criteria for the capacity for glass formation T_x / T_l and d_c (Fig. 1*c*, *g*) shows that the T_x / T_l criterion for AA of the Ti_2Ni–Zr_2Ni section reacts very little to considerable changes in the critical cooling rate of the melts.

The special role of the ternary Laves phase ZrTiNi in the formation of AA can be seen from the characteristic salient points on the constitution–properties diagrams (ρ and H_V) in the range of phase homogeneity (Fig. 1 *d*, *e*) which corresponds to the presence of chemical short-range order and possible formation in the melt of the ternary associate [9] corresponding to that composition. X-ray diffraction analysis also indicates the special character of the short-range order of AA with 17·7, 26·7 and 30% Zr, which belong to the homogeneity range of the λ_1 phase. This is particularly obvious in the region of the second halo of the structure factor. In contrast to the usual shape, with a branch on the high S value side, which is observed in various different AA, the second halo of the structure factor $A(S)$ of those alloys is "spread" over several subpeaks (Fig. 2). On the $A(S)$ curve for AA with 17·7 and 30% Zr there are three distinct subpeaks. The main one in the region of the second halo corresponds to S values of 4·45–4·5 Å^{-1}, the second is in the range 4·85–4·90 Å^{-1} and the third 5·20–5·25 Å^{-1}. The complexity of that structure factor in the λ_1 phase range requires further investigation. In our case the similarity of the short-range order curves for AA containing 17·7, 26·7 and 30% Zr, and the difference between them and the AA corresponding to compounds Ti_2Ni and Zr_2Ni, correlates very well with the nonmonotonic variation in the properties of alloys of that section.

The mean coordination number $<Z>$ also varies nonmonotonically as a function of the composition of those AA, reaching a peak at 15·2–15·4 for compositions 17·7–30% Zr. For AA corresponding to intermetallic compounds Ti_2Ni and Zr_2Ni $<Z>$ is 14·2 and 14·5 respectively.

By analogy with inorganic glasses [10], we can take it that the above features indicate that Laves phase ZrTiNi is a strong glass former. The high glass-forming capacity is due to the chemical nature of the phase (the presence of icosahedral coordinations). In the melt, there may be local atomic stacking patterns in the structure of the Laves phase, and that is reflected by the properties of the AA.

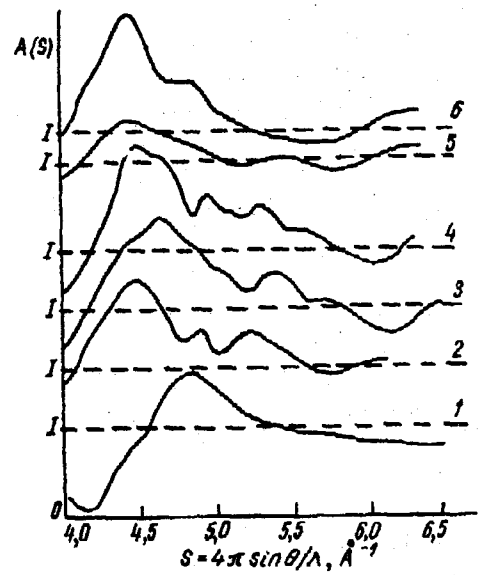

Fig. 2. Region of the second halo of the structure factor of AA of the Ti_2Ni–Zr_2Ni section: *1* — 6·6, *2* — 17·7, *3* — 26·7, *4* — 30, *5* — 46·7, *6* — 66·7% Zr.

An important question in the phase–glass former concept is that of their interaction. According to these results an increase in the glass-forming capacity of the alloys must be due to two factors, i.e. the size and competition of the clusters formed between phases and glass formers. The effect of the first factor can be seen on compounds Ti_2Ni and ZrTiNi for which the Haffner rule [11] obtains, i.e. that the capacity of alloys to amorphization increases when a chemical compound AB_2 is alloyed with an element with a larger atomic radius (in our case Zr). A big increase in glass-forming capacity (R_c = 8.10^3 K/sec) is observed in the range of eutectic ZrTiNi–Zr_2Ni, and could be due to the simultaneous effect of those two factors. X-ray diffraction analysis of eutectic AA shows their structure to be different from that of AA which crystallize with a λ_1 phase structure (17–30% Zr), and of compound Zr_2Ni. The second halo of the structure factor is in the usual shape for AA, with a branch on the large *S* side. First peak of the radial atomic distribution function is not split into two subpeaks as is the case for the AA Zr_2Ni.

Thus it can be said that the AA in question do not possess the pronounced short-range order corresponding to a λ_1 or *l* phase, only having a mixture of regions with short-range order of one or the other type.

REFERENCES

1. Yu. K. Kovneristyy, E. K. Osipov and Ye. A. Trofimova, *Fiziko-khimichestiye osnovy sozdaniya amorfnykh metallicheskikh splavov* (*Physico-chemical Principles of the Creation of Amorphous Metallic Alloys*), Moscow, Nauka, 114 (1983).
2. N. D. Nabitovich, L. I. Stetsiv and Ya. V. Voloshchuk, (Determination of coherent intensity and background intensity from the experimental curve of electron scattering), *Kristallografiya*, **12**, 584 (1967).
3. E. Babich, Z. Maronich, D. Pavuna and V. Leontich, (Analysis of the resistivity of amorphous alloy $Fe_{40}Ni_{40}B_{20}$ during phase transformations), in: *Bystrozakalennye metally* (*Rapidly Quenched Metals*) Ed. B. Kantov, Moscow, Metallurgiya, 196 (1983).
4. K. Suzuki, H. Fujimori and K. Hasimoto, *Amorphous Metals*.
5. M. Hagiwara, A. Inoe and T. Masumoto, The critical thickness for the formation of Fe-, Ni- and Co-based amorphous alloys with metalloids, *The Science Reports of the Res. Inst. Tōh. Univ.*, **A29**, 351 (1981).
6. N. Hansen and K. Anderko, *Structure of Binary Alloys*.

7. V. K. Grigorovich (The chemical bond in metalloids), in: *Stroyeniye, svoystva i primeneniye metallidov* (*Structure, Properties and Application of Metalloids*), Moscow, Nauka, 26 (1974).
8. G. A. Davis, *Fast Quenching Methods and the Formation of Amorphous Metallic Alloys.*
9. F. Sommer, *The Model of Associates in the Theory of Molten Alloys.*
10. A. Felz, *Amorphous and Glass-forming Inorganic Solids.*
11. *Metallic Glasses. Ionic structure, electron transport and crystallization.* Ed. G. I. Gunther and G. Beck.